

THE WORLD IS NOT MONO: ENABLING SPATIAL UNDERSTANDING IN LARGE AUDIO-LANGUAGE MODELS

Anonymous authors

Paper under double-blind review

ABSTRACT

Existing large audio-language models perceive the world as "mono"—a single stream of audio that ignores the critical spatial dimension ("where") required for universal acoustic scene analysis. To bridge this gap, we first introduce a hierarchical framework for Auditory Scene Analysis (ASA). Guided by this framework, we introduce a system that enables models like Qwen2-Audio to understand and reason about the complex acoustic world. Our framework achieves this through three core contributions: First, we build a large-scale, synthesized binaural audio dataset to provide the rich spatial cues. Second, we design a hybrid feature projector, which leverages parallel semantic and spatial encoders to extract decoupled representations. These distinct streams are integrated via a dense fusion mechanism, ensuring the model receives a holistic view of the acoustic scene. Finally, we employ a progressive training curriculum, advancing from supervised fine-tuning (SFT) to reinforcement learning via Group Relative Policy Optimization (GRPO), to explicitly evolve the model's capabilities towards reasoning. On our comprehensive benchmark, the model demonstrates comparatively strong capability for spatial understanding. By enabling this spatial perception, our work provides a clear pathway for leveraging the powerful reasoning abilities of large models towards holistic acoustic scene analysis, advancing from "mono" semantic recognition to spatial intelligence.

1 INTRODUCTION

The expansion of Large Language Models (LLMs) from text-centric processing to multimodal intelligence has brought renewed attention to the auditory domain. Recent Large Audio-Language Models (LALMs) have demonstrated remarkable capabilities in understanding and following instructions related to the semantic content of audio—the 'what' in speech, general sounds, and music (Chu et al., 2024; Yang et al., 2024). However, prevailing LALM frameworks predominantly treat audio as a monophonic time series, lacking explicit modeling of spatial attributes—the 'where'. Technical reports and public benchmarks for these models rarely address reasoning about direction, distance, or spatial relationships, a gap that constitutes the primary motivation for our work.

To formalize and systematically address this gap, we introduce a novel three-layer cognitive framework for Auditory Scene Analysis (ASA). Our framework is inspired by classic cognitive models in the field of Computational Auditory Scene Analysis (CASA), particularly Albert Bregman's two-stage theory of human auditory perception, which distinguishes between data-driven "Primitive Grouping" and knowledge-driven "Schema-based Grouping" (Bregman, 1990). We propose that genuine auditory intelligence requires progressing through three sequential levels of capability:

- **L1: Static Identification:** The foundational perceptual layer, responsible for identifying the discrete properties of individual sounds (e.g., their semantic class, 'what', and their spatial location, 'where').
- **L2: Relational Integration:** The relational aggregation layer, responsible for associating or "binding" these disparate attributes into a single, coherent auditory object (e.g., knowing *that specific* 'dog bark' came from *that specific* 'left-hand' location).
- **L3: Cognitive Reasoning:** The high-level cognitive layer, which uses the bound objects from L2 and world knowledge ('schemas') to infer complex relationships, causality, and scene context.

054 Using this framework, we can clarify the current limitation: existing LALMs are largely confined to
055 the *semantic-half* of L1, while almost completely lacking the *spatial-half* of L1, as well as L2 and
056 L3 capabilities.

057 This disregard for spatial dimensions starkly contrasts with the fundamental mechanisms of biolog-
058 ical hearing. As established in classical auditory scene analysis, the brain leverages binaural cues,
059 such as Interaural Time Differences (ITD) and Interaural Level Differences (ILD), to localize sound
060 sources and segregate auditory streams. This process provides a "spatial release from masking" and
061 underpins the 'cocktail party effect,' enabling focused listening in complex acoustic environments.
062 A model incapable of processing these binaural cues is, in a perceptual sense, "spatially deaf," re-
063 sponding only to a one-dimensional projection of a three-dimensional sound field.

064 This limitation imposes significant constraints on real-world applications in robotics, augmented
065 reality, and assistive hearing, all demanding a joint understanding of audio's content and spatial ar-
066 rangement. Recent explorations have begun extending the "encoder-to-LLM" paradigm to spatial
067 audio, typically by processing binaural signals or Ambisonics recordings (You et al., 2025). For
068 instance, BAT(Zheng et al., 2025) introduced spatial question answering, while subsequent meth-
069 ods improved reasoning by decoupling spatial features or using contrastive learning for localization
070 (Devnani et al., 2024). Despite these promising first steps, the research landscape remains fractured,
071 with most large-scale models focused on semantics (Tang et al., 2024; Huang et al., 2023) while
072 specialized systems handle spatial physics (Shimada et al., 2021). We propose to bridge this di-
073 vide, using the reasoning core of an LLM to unify these capabilities and process open-ended spatial
074 queries with physically consistent representations.

075 However, the primary bottleneck to integrating spatial awareness into general auditory intelligence
076 is not the lack of algorithmic starting points, but the scarcity of appropriate data and representations.
077 Large-scale audio datasets like FSD50K (Fonseca et al., 2022), Clotho (Drossos et al., 2019), and
078 MusicCaps (Agostinelli et al., 2023b) are rich in semantic labels but lack the binaural or 3D spatial
079 metadata required for joint semantic-spatial alignment. Real-world spatial data, while valuable,
080 remains limited in scale and diversity. Consequently, physically-consistent procedural simulation
081 emerges as the most viable path forward. Tools such as Pyroomacoustics (Scheibler et al., 2017)
082 and high-resolution Head-Related Transfer Function (HRTF) databases (Audio Engineering Society,
083 2015) enable the systematic generation of large-scale training corpora with complete "position-
084 semantic-environment" annotations.

085 In this context, we introduce **The World is Not Mono (TWNM)**, a framework that extends LALMs
086 from semantic recognition to spatial reasoning by integrating synthetic binaural data, specialized
087 representation learning, and reinforcement learning alignment.

088 **Contributions.** The main contributions of this work are:

- 089 • **Synthetic binaural data pipeline:** construction of a scalable simulation framework using phys-
090 ically realistic Binaural Room Impulse Responses (BRIRs) / Head-Related Transfer Functions
091 (HRTFs) to generate large-scale, spatially annotated audio-language QA pairs across diverse en-
092 vironments.
- 093 • **Hybrid Feature Projector:** design of a dual-stream projection framework that explicitly decou-
094 ples semantic and spatial processing using specialized expert layers, integrated via a dense fusion
095 mechanism for feature alignment.
- 096 • **Training and alignment:** a progressive curriculum that first optimizes [the projector and expert](#)
097 [layers](#) with the LLM frozen, followed by joint fine-tuning. To further align spatial reasoning with
098 natural language, GRPO (Shao et al., 2024) is employed, using rule-based rewards and relative
099 advantages to improve output accuracy in multiple-choice spatial QA tasks.
- 100 • **Comprehensive evaluation:** demonstration of robust spatial understanding and relational reason-
101 ing on our promoted benchmarks, highlighting a viable path for spatially aware LALMs.

102 This work positions spatial perception not as an incremental feature, but as a fundamental dimension
103 essential for achieving genuine auditory intelligence. The remainder of the paper is organized as
104 follows: Section 2 reviews prior efforts on LALMs, spatial audio modeling, and data synthesis.
105 [Section 3 shows the problem formulation of ASA.](#) Section 4 introduces our proposed framework.
106 Section 5 presents evaluation results on our proposed benchmark. Finally, Section 6 concludes with
107 discussions and future directions.

2 RELATED WORK

Large Audio-Language Models Foundation models such as Qwen2-Audio (Chu et al., 2024), SALMONN (Tang et al., 2024), and AudioGPT (Huang et al., 2023) unify speech, sound, and music under a language interface, but remain focused on semantic tasks. Most benchmarks neglect localization and spatial reasoning, leaving models unable to process direction or distance.

Spatial Audio and LLMs Recent efforts extend the encoder-to-LLM paradigm to spatial audio. BAT(Zheng et al., 2025) evaluated binaural reasoning on the SpatialSoundQA benchmark, and ELSA aligned spatial audio and text via contrastive learning (Devnani et al., 2024). These approaches show potential but leave representation design and training strategies unresolved.

Computational Auditory Scene Analysis (CASA) SELD methods using FOA input, e.g., ACC-DOA (Shimada et al., 2021) and STARSS23 (Shimada et al., 2023), jointly predict sound class and direction. While effective for structured outputs, they mismatch the open-vocabulary and conversational style of LALMs, and early QA adaptations remain limited.

Data Synthesis Because large-scale spatially annotated corpora are scarce, benchmarks often rely on simulation. SpatialSoundQA, for example, renders binaural or FOA mixtures by convolving clean sources with room responses. Public content sets such as FSD50K (Fonseca et al., 2022), Clotho (Drossos et al., 2019), and MusicCaps (Agostinelli et al., 2023b), combined with tools such as Pyroomacoustics (Scheibler et al., 2017) and standardized HRTFs (Audio Engineering Society, 2015), provide reproducible pipelines, though still narrower in scope than large semantic datasets.

Training Paradigms Scaling and alignment methods from general-purpose LLMs also inform spatial modeling. MoE architectures (Fedus et al., 2022; Lepikhin et al., 2020) allow efficient specialization, while reinforcement learning techniques such as GRPO (Shao et al., 2024) refine reasoning and output formats. However, their application to spatial audio remains at an early stage.

3 TASK DEFINITION OF AUDITORY SCENE ANALYSIS

We define ASA by deconstructing the task into three distinct layers: Static Identification (\mathcal{L}_1), Relational Quantification (\mathcal{L}_2), and Cognitive Reasoning (\mathcal{L}_3). This framework aligns with classical theoretical research in auditory scene analysis and aims to provide guidance for the construction of machine auditory frameworks.

3.1 PRELIMINARIES AND DEFINITIONS

We define an auditory scene \mathcal{S} as a composition of atomic units governed by physical laws and semantic rules.

Objects (\mathcal{O}): Let $\mathcal{O} = \{o_1, \dots, o_N\}$ be the set of perceived auditory objects. Each object o_i is defined by a disentangled attribute tuple:

$$o_i = (c_i, \tau_i, \mathbf{s}_i)$$

where $c_i \in \mathcal{C}$ denotes the semantic class (distinguishing foreground events o^e from background o^{env}), $\tau_i = [t_{start}, t_{end}] \in \mathbb{R}^2$ denotes the temporal span, and $\mathbf{s}_i = (\phi, \theta, d) \in \mathbb{R}^3$ represents spatial coordinates.

Knowledge Base (\mathcal{K}): We assume access to a global knowledge base \mathcal{K} containing physical laws, schemas, and causal graphs, serving as priors for high-level reasoning.

3.2 LAYER 1: STATIC IDENTIFICATION (\mathcal{L}_1)

The foundational layer \mathcal{L}_1 targets atomic perception, mapping the raw waveform $\mathbf{x} \in \mathbb{R}^T$ to a set of discrete, statistically independent entities without inferring higher-order dependencies. Formally, the output is:

$$\mathcal{O}_{\mathcal{L}_1} = \{o_1, o_2, \dots, o_N, o_{env}\}$$

This layer executes attribute extraction across three dimensions: **Semantic Classification** (c) maps segments to labels, distinguishing discrete sound actions (o^e) from global scenes (o^{env}); **Temporal Segmentation** (τ) localizes energy boundaries to define existence intervals $[t_{start}, t_{end}]$; **Spatial Localization** (s) estimates physical coordinates s_i relative to the observer.

3.3 LAYER 2: RELATIONAL INTEGRATION (\mathcal{L}_2)

\mathcal{L}_2 constructs a structured scene graph $\mathcal{G} = (\mathcal{O}, \mathcal{E})$ by integrating relationships. Without high-level logic, this layer focuses on **Attribute Binding** and **Metric Measurement**. The output is a set of relational facts $\mathcal{F}_{rel} = \{r_{ij}, \forall i, j\}$, transforming the list \mathcal{O} into a connected graph.

Intra-Object Binding: To solve the binding problem, we define a query function $Q(o_i)$ that verifies if distinct features belong to the same entity. Given observed attributes \mathbf{a} , it regresses missing $\bar{\mathbf{a}}$:

$$P(\bar{\mathbf{a}} | \mathbf{a}, \mathbf{x}) \rightarrow \hat{\mathbf{a}}$$

This enables cross-modal inference, such as $c \rightarrow \tau, \mathbf{s}$ or $\mathbf{s}, \tau \rightarrow c$.

Inter-Object Relations: We define edges \mathcal{E} as quantifiable interactions via operators ψ_k :

$$r_{ij} = \psi_k(o_i, o_j) \in \mathbb{R}^d$$

Relations capture physical and structural interactions: For **Environment-Event** interactions, physical modifications (e.g., reverb, occlusion) and perceptual interactions (e.g., masking) are widely observed; while for **Event-Event** interactions, spatiotemporal structure (e.g., overlap, precedence) and spectral similarity (e.g., harmonic relations) should be detected and measured.

3.4 LAYER 3: COGNITIVE REASONING (\mathcal{L}_3)

The apex layer \mathcal{L}_3 integrates atomic facts (\mathcal{L}_1) and the relational graph (\mathcal{L}_2) with the knowledge base \mathcal{K} . It performs probabilistic inference to derive high-level judgments \mathcal{J} :

$$\mathcal{J}^* = \underset{\mathcal{J}}{\operatorname{argmax}} P(\mathcal{J} | \mathcal{G}, \mathcal{K})$$

This layer supports four advanced reasoning modes:

- **Abductive & Causal Inference:** Distinguishes correlation from causality (e.g., sequential impacts) and infers global context from local evidence (e.g., vehicle sounds \rightarrow “traffic”).
- **Deductive & Commonsense Validation:** Validates perception using physical constraints (e.g., material properties from impact) and detects semantic anomalies via environmental priors.
- **Inductive & Analogical Generalization:** Generalizes recurring structures (e.g., alternating vocals \rightarrow “dialogue”) and characterizes unknown sources via physical analogy (e.g., Doppler \rightarrow motion).
- **Multi-hop Traversal & Metacognition:** Executes graph traversal for complex queries (e.g., temporal search) and performs metacognitive tasks like counterfactual reasoning (e.g., no response \rightarrow “empty”).

Note. The ASA framework defines objects as disentangled tuples (c, τ, \mathbf{s}) . However, solving the spatial-semantic binding problem is a prerequisite for holistic perception. Therefore, this paper specifically focuses on the integration of semantic (c) and spatial (\mathbf{s}) dimensions. We assume the input audio represents a coherent scene or event window, treating τ as an implicit context rather than an explicit prediction target in this stage.

4 METHODOLOGY

4.1 PROBLEM FORMULATION AND DESIGN PRINCIPLES

We address the task of conditional text generation from binaural audio input. Given a two-channel audio waveform $x \in \mathbb{R}^{B \times 2 \times T}$ and a natural language prompt p , the model’s objective is to generate

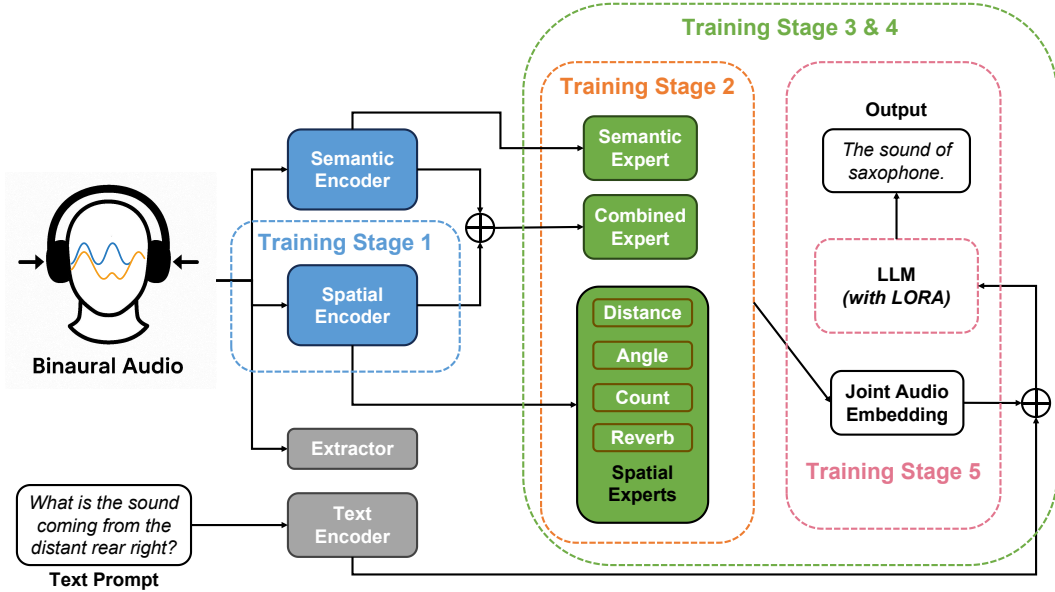


Figure 1: Model Architecture

a textual response y . To enable the model to comprehend not only the semantic content (“what”) but also the spatial arrangement (“where”) of the acoustic scene, we explicitly decompose the audio representation into two distinct components: a semantic embedding $z_{\text{sem}}(x)$ and a spatial embedding $z_{\text{sp}}(x)$. These representations are conditionally fused before being processed by the language decoder:

$$y \sim p_{\theta}(\cdot \mid \text{fuse}(z_{\text{sem}}(x), z_{\text{sp}}(x)), p).$$

Our framework is built upon three core design principles:

- **Decouple-and-Fuse.** Semantic and spatial attributes are modeled by independent, robust encoders. Their outputs are then integrated via a dense fusion mechanism. Unlike sparse routing approaches that may select partial information, our dense fusion ensures that the Language Model receives a complete, simultaneous view of both semantic identity and spatial location.
- **Minimally Invasive LLM Interfacing.** We avoid complex prompt templates and modifications to the LLM’s native tokenization or positional encoding schemes. The final audio representation is simply appended to the prompt embeddings as a suffix, ensuring maximum compatibility with standard autoregressive frameworks.
- **Progressive Curricular Optimization.** We employ a multi-stage training curriculum that proceeds from representation learning to alignment and finally to policy optimization. This disentangles conflicting learning objectives and stabilizes the training of the composite model.

4.2 MODEL ARCHITECTURE

Our architecture, depicted in Figure 1, implements our “Decouple-and-Fuse” principle. The process begins as the input binaural audio is fed into two parallel backbones: a Semantic Encoder to extract a content representation (W) and a Spatial Encoder for locational cues (S'). These decoupled representations are then processed and integrated by our hybrid feature projector. This module employs a set of parallel expert pathways to project features into specialized physical subspaces, followed by a dense fusion layer that unifies them into a comprehensive audio embedding (H_{enc}). This embedding is appended to the prompt embeddings and passed to the LLM decoder for text generation.

Semantic and Spatial Encoders. For semantic feature extraction, we use a frozen Whisper encoder. To specifically isolate content, the binaural input is downmixed to mono by averaging the left and right channels. This process yields a semantic sequence $W \in \mathbb{R}^{B \times L \times 768}$.

For spatial features, we adapt the dedicated encoder from (Wu et al., 2025). It processes the complex STFT of the binaural signal to preserve phase information crucial for localization. The model alternates between frequency-band modeling and temporal modeling using self-attention. Critically, an attractor-based aggregation mechanism allows it to handle a variable number of sound sources. The final output is projected and resampled into a spatial feature sequence $S' \in \mathbb{R}^{B \times L \times 768}$, aligned with the semantic features.

Hybrid Feature Projector. The hybrid feature projector serves as the bridge between the decoupled representations and the decoder. It adopts a "split-transform-merge" strategy to maintain the integrity of specific acoustic attributes while providing a unified context to the LLM.

Parallel Expert Pathways. Instead of a generic linear projection, we employ a set of parallel feed-forward networks, termed "Expert Pathways," to explicitly model distinct acoustic properties. The module comprises:

- **Semantic Pathway** (E_{sem}): Processes the semantic representation W to align content features with the LLM space.
- **Spatial Pathways** ($\{E_{\text{sp}}^{(k)}\}_{k=1}^4$): Process the spatial representation S' . These pathways are specialized to extract distinct spatial attributes: direction, distance, room acoustics (reverberation), and source count. This explicit separation provides a strong inductive bias, ensuring that critical physical cues are preserved and highlighted before fusion.

Dense Feature Fusion. To avoid the information loss associated with sparse routing, we employ a dense fusion mechanism. The outputs of all expert pathways are concatenated to form a rich, multi-view representation, which is then projected by a fusion MLP into the final hidden state H_{enc} . Formally, let $O_{\text{sem}} = E_{\text{sem}}(W)$ and $O_{\text{sp}}^{(k)} = E_{\text{sp}}^{(k)}(S')$. The fusion process is defined as:

$$H_{\text{enc}} = \text{MLP}_{\text{fuse}} \left(\text{Concat} \left[O_{\text{sem}} ; O_{\text{sp}}^{(1)} ; O_{\text{sp}}^{(2)} ; O_{\text{sp}}^{(3)} ; O_{\text{sp}}^{(4)} \right] \right) \in \mathbb{R}^{B \times L \times d_{\text{dec}}}$$

This dense architecture ensures that for every audio token, the LLM has simultaneous access to the full spectrum of semantic and spatial information, facilitating the learning of complex cross-modal dependencies (binding).

LLM Interface. We employ the Qwen2-Audio 7B model as the language decoder. Its core parameters are kept frozen, and we use Low-Rank Adaptation (LoRA)(Hu et al., 2022) for parameter-efficient fine-tuning, applied only to the attention projection matrices (e.g., `q_proj`, `v_proj`). Following our principle of minimal intrusion, the audio hidden state H_{enc} is directly appended to the prompt embeddings $E(p)$, forming the input sequence $[E(p); H_{\text{enc}}] \in \mathbb{R}^{B \times (L_p + L) \times d_{\text{dec}}}$. This simple and robust protocol eliminates the need for prompt engineering.

4.3 LEARNING: A PROGRESSIVE CURRICULUM FROM REPRESENTATION TO POLICY

To disentangle competing learning objectives, we adopt a five-stage curriculum. The input protocol and tokenization remain consistent across all stages to prevent training-inference mismatch.

Stage 1: Encoder Pretraining. In this preparatory stage, only the spatial encoder is trained. The objective is to learn a robust and general-purpose representation of spatial acoustics from a large-scale (potentially unlabeled) binaural audio dataset. This endows the encoder with a strong inductive bias for physical acoustic properties, decoupling this representation learning from the more complex cross-modal alignment task.

Stage 2: Projector Alignment (Alignment I). The audio encoders and the LLM are frozen, and only the hybrid feature projector (Expert Pathways and Fusion MLP) is trained. The optimization is driven by the standard cross-entropy loss \mathcal{L}_{CE} on the decoder output. The goal of this stage is to initialize the projection subspaces and align the fused audio representations with the pre-trained LLM's embedding space without altering the reasoning core.

Stage 3: SFT 1.0 (Alignment II). The encoders remain frozen, while the feature projector and the decoder’s LoRA weights are trained jointly. The objective is to minimize \mathcal{L}_{CE} . This stage focuses on bridging the modality gap between the fused audio representations and the LLM’s latent space, refining the cross-modal interface.

Stage 4: SFT 2.0 (Formatting). In this stage, the encoders remain frozen, while the projector and the decoder’s LoRA weights continue to be trained jointly. The key change is the shift in data distribution towards chain-of-thought samples. The optimization is driven solely by the cross-entropy loss \mathcal{L}_{CE} . The purpose is to transition the model to end-to-end learning, fostering a co-evolution of the reasoning strategy and the desired output format (e.g., `<think>...</think><answer>...</answer>`).

Stage 5: GRPO Preference Optimization. Finally, only the LoRA weights are updated using GRPO. For each sample, we generate a group of m candidate responses $\{y_i\}_{i=1}^m$ from the current policy π_θ . Each response is scored by a reward function:

$$R(y) = R_{\text{fmt}}(y) + R_{\text{ans}}(y).$$

Here, R_{fmt} assesses structural compliance (e.g., proper tag closure), while R_{ans} measures correctness by parsing the content within the `<answer>` tag. GRPO uses the in-batch group mean as a baseline to compute the advantage:

$$A_i = \frac{R(y_i) - \frac{1}{m} \sum_{j=1}^m R(y_j)}{\text{std}_{j=1}^m(R(y_j))}$$

The policy is then updated by maximizing the following objective:

$$\mathcal{L}_{\text{GRPO}}(\theta) = \mathbb{E}_{(x,p), \{y_i\} \sim \pi_\theta} \left[\sum_{i=1}^m \log \pi_\theta(y_i | x, p) \cdot \text{stop_gradient}(A_i) \right].$$

Keeping the encoders and projector frozen during this stage confines the optimization to the small set of LoRA parameters, ensuring stability and efficiency.

In summary, our methodology combines a decoupled representation with a progressive training curriculum to efficiently instill spatial reasoning into a pre-trained LALM.

5 EXPERIMENTS

This section details the experimental evaluation of our framework. We aim to validate the effectiveness of the Hybrid Feature Projector and the progressive curriculum in endowing LALMs with hierarchical spatial intelligence, moving from atomic perception (\mathcal{L}_1) to relational integration (\mathcal{L}_2) and complex reasoning (\mathcal{L}_3).

5.1 DATASETS AND SIMULATION PIPELINE

Lacking suitable public datasets for spatial audio reasoning, we developed a scalable simulation pipeline to generate data for our SFT and GRPO stages. The pipeline combines physically principled BRIR generation with dynamic scene synthesis. We construct diverse acoustic environments by varying room dimensions, wall absorption coefficients, and source positions. Detailed simulation parameters and geometric configurations are provided in Appendix A.

5.2 TRAINING SETUP

Our training regimen follows the progressive curriculum outlined in Section 4, beginning with Projector Alignment, followed by Supervised Fine-Tuning (SFT), and culminating in GRPO. We use LoRA for parameter-efficient fine-tuning and employ the AdamW optimizer. Complete hyperparameters, including learning rates, batch sizes, and hardware specifications, are detailed in Appendix B.

5.3 BENCHMARK CONSTRUCTION

To rigorously evaluate spatial reasoning, we constructed a 1,000-question multiple-choice benchmark using an LLM-powered pipeline. Crucially, the questions are designed to map directly to our proposed ASA framework:

- \mathcal{L}_1 **Perception (32.1%)**: Tasks focusing on atomic identification, such as source counting, semantic recognition, and absolute localization.
- \mathcal{L}_2 **Integration (28.5%)**: Tasks requiring attribute binding, such as associating a specific sound event with a specific location or linking environmental cues to source properties.
- \mathcal{L}_3 **Reasoning (39.4%)**: Tasks involving high-level inference, such as counterfactual reasoning and summarizing the global scene context.

Detailed prompt templates for benchmark generation are provided in Appendix C.

5.4 MAIN RESULTS

To contextualize the performance of TWNM, we compare it against BAT (Zheng et al., 2025), a representative state-of-the-art baseline. Since BAT lacks the capability to generate structured chain-of-thought outputs, we adopted a hybrid evaluation protocol. For \mathcal{L}_1 Perception, we evaluated BAT using direct generation. For complex \mathcal{L}_3 Reasoning and \mathcal{L}_2 Integration tasks, we converted the multi-choice questions into boolean (True/False) discrimination tasks for each option and report the "Per-Option Accuracy". Note that for this binary metric, a random guess yields 50%, whereas standard MCQA accuracy for our model has a random baseline of 25%.

As shown in Table 1, the baseline BAT achieves only 36.40% on \mathcal{L}_3 tasks—well below the random chance threshold of 50%. This indicates that without explicitly decoupled spatial representations, generic LALMs suffer from systematic hallucinations. In contrast, our model, equipped with the Hybrid Feature Projector and Dense Fusion, achieves robust performance (79.60%) on the stricter MCQA metric, validating the necessity of our architecture for high-level reasoning.

Table 1: Comparative results and ablation study across ASA levels. Accuracy (%) is reported for the baseline (BAT) and each stage of our curriculum. BAT’s performance on \mathcal{L}_2 and \mathcal{L}_3 is reported as Per-Option Belief Accuracy (random=50%), while ours is MCQA Accuracy (random=25%). The progressive curriculum yields significant gains, particularly in \mathcal{L}_3 Reasoning.

Competency Area	BAT (Zheng et al., 2025)	SFT 1.0	SFT 2.0	GRPO
Perception (\mathcal{L}_1)	24.57	40.72	62.36	61.05
Integration (\mathcal{L}_2)	35.52 [†]	63.12	56.17	57.75
Reasoning (\mathcal{L}_3)	36.40 [†]	43.64	66.89	79.60
Overall Accuracy	32.50	48.15	63.00	68.69

[†] Denotes Per-Option Accuracy (Binary T/F) where random baseline is 50%.

Our curriculum constitutes a staged ablation where each phase contributes a distinct capability. Moving from base alignment (SFT 1.0) to full instruction tuning (SFT 2.0) and finally to preference optimization (GRPO), overall accuracy rises from 48.15% to 68.69%.

The Evolution of Reasoning (\mathcal{L}_3). Preference optimization yields the largest gains on complex reasoning tasks, which jump from 43.64% (SFT 1.0) to 79.60% (GRPO). Specifically, the scene summarization task reaches 97.22% accuracy, and causal intent reasoning attains 92.00%. This confirms that while SFT 1.0 establishes the physical grounding, the combination of Chain-of-Thought (SFT 2.0) and GRPO is essential for unlocking high-level cognitive analysis.

The Perception-Integration Trade-off. We observe an interesting dynamic in \mathcal{L}_2 Integration tasks. SFT 1.0 achieves the highest performance (63.12%) in this category, outperforming subsequent stages. We interpret this as a trade-off: SFT 1.0 is optimized for direct, mechanical feature binding via the Dense Fusion mechanism. The transition to SFT 2.0 introduces complex language generation, which significantly boosts semantic perception (\mathcal{L}_1 , 40.7% \rightarrow 62.4%) and reasoning, but

432
433
434
435
436
437
438
439
440
441
442
443
444
445
446
447
448
449
450
451
452
453
454
455
456
457
458
459
460
461
462
463
464
465
466
467
468
469
470
471
472
473
474
475
476
477
478
479
480
481
482
483
484
485

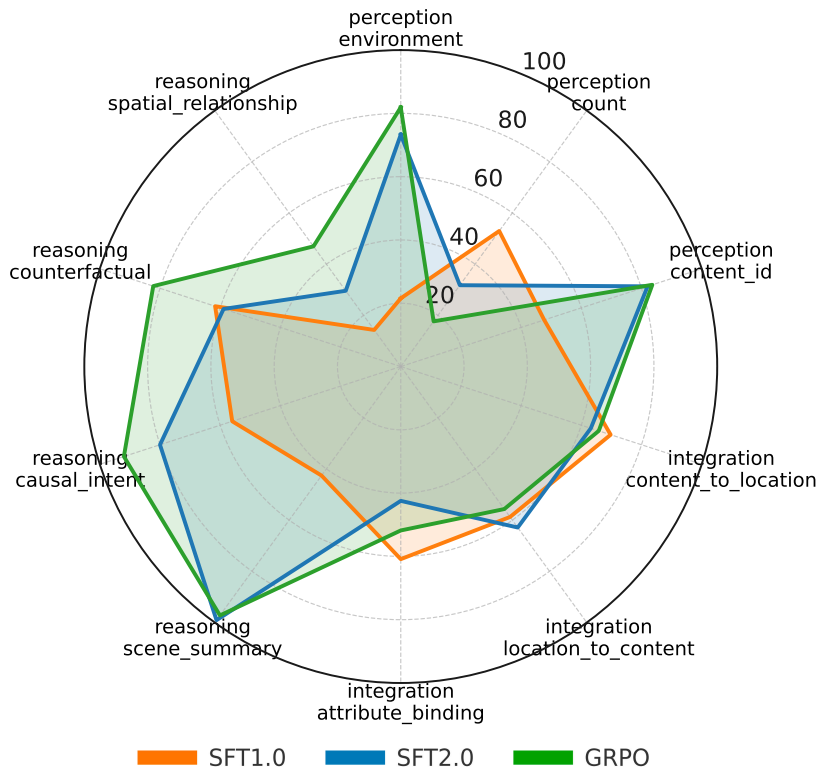


Figure 2: Task-wise accuracies on the ten benchmark categories for SFT1.0, SFT2.0, and GRPO.

incurs a temporary alignment tax on low-level binding precision (63.1% \rightarrow 56.2%). GRPO successfully recovers some of this capability (56.2% \rightarrow 57.8%) while maintaining peak reasoning performance.

Remaining Challenges. While the model excels at spatial semantics, the *Perception Count* task remains challenging, dropping to 17.65% in the final stage. This suggests that while LALMs are excellent at qualitative spatial reasoning (e.g., "farther", "left of"), fine-grained numeracy remains an open challenge for end-to-end audio models.

6 CONCLUSION

In this work, we addressed the critical limitation of existing Large Audio-Language Models—their inability to perceive spatial audio—by introducing **The World is Not Mono (TWNM)**. Guided by our proposed hierarchical Auditory Scene Analysis (ASA) framework, this system bridges the gap between single acoustic tasks and cognitive reasoning. We demonstrated that a combination of large-scale synthetic binaural data, a hybrid feature projector utilizing dense fusion, and a progressive SFT-to-GRPO curriculum can successfully endow LALMs with robust spatial reasoning. Our experiments validated the superiority of the dense fusion mechanism over unified baselines, while preference optimization proved decisive for mastering complex reasoning. By moving beyond the mono paradigm, our work establishes a clear pathway for three-dimensional auditory intelligence. Future work will focus on enhancing the model’s generalization to diverse in-the-wild recordings and extending our framework to support multi-channel formats like Ambisonics, further broadening its applications in embodied AI, augmented reality, and assistive technologies.

7 ETHICS STATEMENT

All authors of this paper have read and adhered to the ICLR Code of Ethics. This research does not involve human subjects, personally identifiable information, or sensitive data. The datasets utilized are publicly available and have been handled in accordance with their specified licenses. While we have strived to ensure the fairness and robustness of our methods, we acknowledge that potential biases may exist in the underlying data, which could be reflected in the model’s performance. We believe the potential societal benefits of this work in advancing the understanding of audio scene analysis outweigh the foreseeable risks. We declare no conflicts of interest.

8 REPRODUCIBILITY STATEMENT

We are committed to ensuring the reproducibility of our research. All datasets used in our experiments are publicly available. For the review period, we include anonymized supplementary materials containing core implementation modules and configuration files to facilitate inspection of our method. A fully runnable codebase with scripts and instructions will be released upon acceptance.

REFERENCES

- Andrea Agostinelli, Timo I. Denk, Zalan Borsos, Jesse Engel, Mauro Verzetti, et al. Musiclm: Generating music from text. *arXiv preprint arXiv:2301.11325*, 2023a.
- Andrea Agostinelli, Timo I. Denk, Zalán Borsos, Jesse Engel, Mauro Verzetti, Antoine Caillon, Qingqing Huang, Aren Jansen, Adam Roberts, Marco Tagliasacchi, Matt Sharifi, Neil Zeghidour, and Christian Frank. Musiclm: Generating music from text, 2023b. URL <https://arxiv.org/abs/2301.11325>.
- Audio Engineering Society. AES69-2015: Aes standard for file exchange—spatial acoustic data file format. AES Standard, 2015. URL <https://www.aes.org/publications/standards/search.cfm?docID=96>.
- Albert S. Bregman. *Auditory Scene Analysis: The Perceptual Organization of Sound*. The MIT Press, 05 1990. ISBN 9780262269209. doi: 10.7551/mitpress/1486.001.0001. URL <https://doi.org/10.7551/mitpress/1486.001.0001>.
- Fabian Brinkmann, Alexander Lindau, Stefan Weinzierl, Gunnar Geissler, Steven van de Par, Markus M’uller-Trapet, and Rogier Opdam. The fabian head-related transfer function data base. DepositOnce, Technische Universit’at Berlin, 2017. URL <https://depositonce.tu-berlin.de/items/3b423df7-a764-4ce1-9065-4e6034bba759>.
- Yunfei Chu, Jin Xu, Qian Yang, Haojie Wei, Xipin Wei, Zhifang Guo, Yichong Leng, Yuanjun Lv, Jinzheng He, Junyang Lin, Chang Zhou, and Jingren Zhou. Qwen2-audio technical report. *arXiv preprint arXiv:2407.10759*, 2024. URL <https://arxiv.org/abs/2407.10759>.
- Bhavika Devnani, Skyler Seto, Zakaria Aldeneh, Alessandro Toso, Elena Menyaylenko, Barry-John Theobald, Jonathan Sheaffer, and Miguel Sarabia. Learning spatially-aware language and audio embeddings, 2024. URL <https://arxiv.org/abs/2409.11369>.
- Konstantinos Drossos, Samuel Lipping, and Tuomas Virtanen. Clotho: An audio captioning dataset, 2019. URL <https://arxiv.org/abs/1910.09387>.
- William Fedus, Barret Zoph, and Noam Shazeer. Switch transformers: Scaling to trillion parameter models with simple and efficient sparsity, 2022. URL <https://arxiv.org/abs/2101.03961>.
- Eduardo Fonseca, Xavier Favory, Jordi Pons, Frederic Font, and Xavier Serra. Fsd50k: An open dataset of human-labeled sound events, 2022. URL <https://arxiv.org/abs/2010.00475>.
- Haorui He, Zengqiang Shang, Chaoren Wang, Xuyuan Li, Yicheng Gu, Hua Hua, Liwei Liu, Chen Yang, et al. Emilia: An extensive, multilingual, and diverse speech dataset for large-scale speech generation. *arXiv preprint arXiv:2407.05361*, 2024. doi: 10.48550/arXiv.2407.05361.

- 540 Edward J Hu, Yelong Shen, Phillip Wallis, Zeyuan Allen-Zhu, Yuanzhi Li, Lu Wang, and Weizhu
541 Chen. Lora: Low-rank adaptation of large language models. *arXiv preprint arXiv:2106.09685*,
542 2022.
- 543 Rongjie Huang et al. Audiogpt: Understanding and generating speech, music, sound, and talking
544 head. *arXiv preprint arXiv:2304.12995*, 2023. URL [https://arxiv.org/abs/2304.](https://arxiv.org/abs/2304.12995)
545 12995.
- 546 Dmitry Lepikhin, HyoukJoong Lee, Yuanzhong Xu, Dehao Chen, Orhan Firat, Yanping Huang,
547 Maxim Krikun, Noam Shazeer, and Zhifeng Chen. Gshard: Scaling giant models with condi-
548 tional computation and automatic sharding, 2020. URL [https://arxiv.org/abs/2006.](https://arxiv.org/abs/2006.16668)
549 16668.
- 550 Samyam Rajbhandari, Jeff Rasley, Olatunji Ruwase, and Yuxiong He. Zero: Memory optimizations
551 toward training trillion parameter models. *arXiv preprint arXiv:1910.02054*, 2020.
- 552 Robin Scheibler, Eric Bezzam, and Ivan Dokmanić. Pyroomacoustics: A python package for audio
553 room simulations and array processing algorithms. *arXiv preprint arXiv:1710.04196*, 2017. URL
554 <https://arxiv.org/abs/1710.04196>.
- 555 Zhihong Shao, Peiyi Wang, Qihao Zhu, Runxin Xu, Junxiao Song, Xiao Bi, Haowei Zhang,
556 Mingchuan Zhang, Y. K. Li, Y. Wu, and Daya Guo. Deepseekmath: Pushing the limits of mathe-
557 matical reasoning in open language models, 2024. URL [https://arxiv.org/abs/2402.](https://arxiv.org/abs/2402.03300)
558 03300.
- 559 Kazuki Shimada, Yuichiro Koyama, Naoya Takahashi, Shusuke Takahashi, and Yuki Mitsufuji. Ac-
560 cdoa: Activity-coupled cartesian direction of arrival representation for sound event localization
561 and detection, 2021. URL <https://arxiv.org/abs/2010.15306>.
- 562 Kazuki Shimada, Archontis Politis, Parthasaarathy Sudarsanam, Daniel Krause, Kengo Uchida,
563 Sharath Adavanne, Aapo Hakala, Yuichiro Koyama, Naoya Takahashi, Shusuke Takahashi, Tu-
564 omas Virtanen, and Yuki Mitsufuji. Starss23: An audio-visual dataset of spatial recordings of real
565 scenes with spatiotemporal annotations of sound events, 2023. URL [https://arxiv.org/](https://arxiv.org/abs/2306.09126)
566 [abs/2306.09126](https://arxiv.org/abs/2306.09126).
- 567 Changli Tang, Wenyi Yu, Guangzhi Sun, Xianzhao Chen, Tian Tan, Wei Li, Lu Lu, Zejun Ma, and
568 Chao Zhang. Salmonn: Towards generic hearing abilities for large language models, 2024. URL
569 <https://arxiv.org/abs/2310.13289>.
- 570 Donghang Wu, Jiaqi Du, Tianshu Qu, Qingbo Huang, and Dejun Zhang. Moving sound source
571 localization and tracking based on envelope estimation for unknown number of sources. 05 2025.
- 572 Qian Yang, Jin Xu, Wenrui Liu, Yunfei Chu, Ziyue Jiang, Xiaohuan Zhou, Yichong Leng, Yuan-
573 jun Lv, Zhou Zhao, Chang Zhou, and Jingren Zhou. AIR-bench: Benchmarking large audio-
574 language models via generative comprehension. In *Proceedings of ACL*, 2024. URL [https://](https://aclanthology.org/2024.acl-long.109.pdf)
575 aclanthology.org/2024.acl-long.109.pdf.
- 576 Yuhuan You, Yufan Qian, Tianshu Qu, Bin Wang, and Xueyang Lv. Spherical harmonic beamform-
577 ing based ambisonics encoding and upscaling method for smartphone microphone array. In *Audio*
578 *Engineering Society Convention 158*. Audio Engineering Society, 2025.
- 579 Zhisheng Zheng, Puyuan Peng, Ziyang Ma, Xie Chen, Eunsol Choi, and David Harwath. Bat:
580 Learning to reason about spatial sounds with large language models, 2025. URL [https://](https://arxiv.org/abs/2402.01591)
581 arxiv.org/abs/2402.01591.
- 582
583
584
585
586
587
588
589
590
591
592
593

594 APPENDIX

595
596 A DATA SIMULATION DETAILS

597 To ensure the diversity and physical realism of our training data, we implemented a comprehensive
600 simulation pipeline governed by the following parameters.

601
602 **Room Acoustics and Geometry.** We generate Binaural Room Impulse Responses (BRIRs) using
603 the `pyroomacoustics` simulator (Scheibler et al., 2017). Rooms are modeled as shoebox shapes
604 with dimensions sampled uniformly from three categories:

- 606 • **Small:** $x \in [3, 5]$ m, $y \in [4, 6]$ m, $z \in [2.5, 3.5]$ m
- 607
- 608 • **Medium:** $x \in [8, 12]$ m, $y \in [10, 15]$ m, $z \in [3, 5]$ m
- 609
- 610 • **Large:** $x \in [20, 30]$ m, $y \in [25, 35]$ m, $z \in [10, 15]$ m

611 Wall absorption coefficients $\alpha \in [0, 1]$ are sampled to simulate varying Reverberation Times (RT60):

- 613 • **High Reverberation (Reflective):** $\alpha \in [0.05, 0.25]$
- 614
- 615 • **Medium Reverberation:** $\alpha \in [0.25, 0.5]$
- 616
- 617 • **Low Reverberation (Absorptive):** $\alpha \in [0.5, 0.95]$

618 For each room, we randomly place one receiver and 30 candidate source positions. The receiver’s
619 Head-Related Transfer Functions (HRTFs) are sourced from the FABIAN dataset (Brinkmann et al.,
620 2017).

621
622 **Source Material and Scene Synthesis.** Audio clips are sampled from FSD50K (Fonseca et al.,
623 2022), Clotho v2 (Drossos et al., 2019), MusicCaps (Agostinelli et al., 2023a), and Emilia (He
624 et al., 2024). These dry clips are convolved with the generated BRIRs, scaled by a random gain,
625 and summed to create the final mixture. This pipeline ensures precise ground-truth labels for \mathcal{L}_1
626 (location, class) and \mathcal{L}_2 (spatial relations) tasks.

627
628 **Data Formats.** The training data evolves across stages:

- 631 • **SFT Data:** The initial stage employs open-ended QA pairs to align the `Feature Projector` with
632 the LLM. The subsequent SFT 2.0 stage introduces Chain-of-Thought (CoT) formatting (using
633 `<think>` and `<answer>` tags) to prime the model for reasoning.
- 634
- 635 • **GRPO Benchmark:** A held-out set of multiple-choice questions designed to probe specific spa-
636 tial competencies, serving as the environment for reinforcement learning.

637
638 B TRAINING IMPLEMENTATION DETAILS

639
640 **Hyperparameters.** We utilize the AdamW optimizer across all training stages. The detailed hy-
641 perparameter configuration for each stage of our progressive curriculum is provided in Table 2.

642
643 **System Configuration.** All experiments were conducted on a cluster of 8 NVIDIA RTX 5090
644 GPUs (32 GB VRAM each). We leverage `torchrun` for distributed training and utilize the Deep-
645 Speed ZeRO Stage 2 strategy (Rajbhandari et al., 2020) with CPU offloading to maximize memory
646 efficiency. The framework is implemented using PyTorch and the Hugging Face Transformers li-
647 brary.

Table 2: Hyperparameter settings for each training stage.

Hyperparameter	Stage 2 (Alignment I)	Stage 3/4 (SFT)	Stage 5 (GRPO)
Learning Rate	1×10^{-4}	5×10^{-5}	1×10^{-6}
Batch Size (Global)	128	128	64
Epochs	2	3	1
Warmup Ratio	0.03	0.03	0.1
Gradient Clipping	1.0	1.0	1.0
LoRA Rank (r)	N/A	8	8
LoRA Alpha (α)	N/A	32	32
Optimizer	AdamW	AdamW	AdamW

C PROMPT FOR BENCHMARK GENERATION

Prompt (for generating open-ended spatial QA)

You are a top-tier AI course designer preparing graduation exam questions for an advanced spatial audio model. This model has already mastered the basics of recognizing sound content (semantic), localizing sources (localization), perceiving the environment (acoustics), and counting (count). Your task: given a `<scene_description>`, design 1–2 **open-ended**, complex questions that require integrating multiple abilities, and provide detailed, fluent, high-quality answers.

[Design Principles]

- **Reject simplicity**: do not ask “Where is the dog?”; instead ask “What is the main activity in the scene, and where does it occur relative to me in space?”
- **Encourage reasoning**: propose questions that require inference from multiple cues. For example: “Based on the room’s reverberation and the sounds inside, what is the most plausible type of place?”
- **Simulate dialogue**: both questions and answers should read like a natural conversation between humans.

[Example] `<scene_description>`

Indoors with slight reverberation, two sounds are audible. One is keyboard typing from straight ahead at a close distance. The other is birdsong coming from outside the window, located up-right and farther away.

`</scene_description>`

`<generated_data>`

```
[
  {
    "instruction": "Based on what you hear, can you infer where I might be and what I'm doing?",
    "answer": "It sounds like you're likely in a room—perhaps an office or at home. The clear, nearby keyboard typing suggests you're working or studying on a computer. Meanwhile, the birdsong from outside implies it's likely daytime and that you're close to a window."
  }
]
```

`</generated_data>`

[Formal Task] `<scene_description>`

`{{ insert RTSD here }}`

`</scene_description>`

`<generated_data>`

`</generated_data>`

D CASE STUDY

To further illustrate the reasoning ability of our model, we present a representative case study drawn from the evaluation set. The task requires the model to infer the most plausible explanation of an acoustic scene based on the perceived spatialized audio.

Ground Truth (Reference)

Scene Description:

- **Scene type:** Mixed, single sound source
- **Sound event:** Respiratory sound (breathing)
- **Azimuth:** 317°, **Elevation:** -13°, **Distance:** 17.4 m
- **Room acoustics:** Anechoic, absorption coefficient ≈ 0.99 , RT60 = 0.0 s

Correct Answer:

A. The listener may be using headphones to hear a specially recorded or processed audio, in which a breathing sound is precisely placed at a specific position in the sound field.

Question

Task: Based on the audio you hear, which of the following explanations is the most reasonable for this scene?

- A. The listener may be using headphones to hear a specially recorded or processed audio, in which a breathing sound is precisely placed at a specific position in the sound field.
- B. In a wide-open space, someone is breathing about 17 meters away from the listener, and the openness of the space makes the sound unusually clear.
- C. The listener is in a completely silent room, and due to over-concentration, hallucinates the distant sound of breathing.
- D. This is a live recording in a large concert hall, where a breathing sound from an audience member was mistakenly amplified during post-production.

Model Output (verbatim)

|<think>| The core of the question is to infer the most reasonable scene based on the heard sound.

First, I analyze the key sound elements in the audio. I heard a clear breathing sound, coming from my front-left, about 17 meters away. The sound is very clear, almost without echo, which indicates I am in an open environment, such as a large space. The sound position is very precise, at azimuth 313 degrees and elevation 1 degree, which shows that the sound source is fixed rather than moving randomly.

Based on these observations, I evaluate each option:

– Option A states that the breathing sound was placed at a specific position. This matches exactly with the sound location I heard (azimuth 313 degrees). A processed audio, where a sound is placed at a specific position in the recording, is entirely possible.

– Option B describes a wide-open space with someone breathing. This contradicts the clear, echo-free sound characteristics. A wide-open space would produce noticeable reverberation.

– Option C suggests that the sound is a hallucination from silence. This is clearly wrong because I distinctly heard a breathing sound.

– Option D suggests a concert hall live recording where the breathing was over-amplified. However, a concert hall should have noticeable reverberation, which is absent here, so D is not reasonable.

In summary, Option A best fits the sound characteristics: a clear, precisely located breathing sound placed in a large space. |</think>|

According to the audio analysis, the sound comes from a precise location in a nearly echo-free large space, indicating that it is likely a processed audio rather than a real-world event.

|<answer>| A |</answer>|

E STATEMENT ON THE USE OF LARGE LANGUAGE MODELS (LLMs)

In the preparation of this manuscript, LLMs were utilized for two distinct purposes. First, as a general-purpose tool for tasks such as grammar correction and language polishing of the manuscript text. Second, as a core component of our methodology, LLMs were employed in a semi-automated

756 pipeline under human supervision to generate the questions and chain-of-thought rationales for our
757 benchmark dataset, as detailed in Section 5.3. The core research ideation, experimental design, and
758 the final analysis were conceived and executed by the authors. We confirm that the LLMs’ role,
759 while integral to the methodology, was that of a tool to implement our research design. The authors
760 take full responsibility for all content presented in this paper, including the validity of the generated
761 benchmark and any potential inaccuracies.

762
763
764
765
766
767
768
769
770
771
772
773
774
775
776
777
778
779
780
781
782
783
784
785
786
787
788
789
790
791
792
793
794
795
796
797
798
799
800
801
802
803
804
805
806
807
808
809